

# The Direction Switching Control of Electromagnetic Waves Based on All-dielectric Metamaterials

Yanan Hua, Kejian Chen\*, Yanjun Fu, and Xiaofan Zhang

Shanghai Key Lab of Modern Optical System

Engineering Research Center of Optical Instrument and System, Ministry of Education  
University of Shanghai for Science and Technology, 516Jungong Road, Shanghai 200093, China

\*ee.kjchen@gmail.com

**Abstract** — Electromagnetic waves control is becoming more and more urgent for important applications in communication and military fields. Studies have shown that it is possible to achieve reflection and refraction control of electromagnetic waves by introducing phase gradient. Wavefront control of electromagnetic waves can be achieved with metamaterials devices. However, metamaterials devices have to be diversified and enhance their capabilities to catch up the rapidly expanding demand on dynamic control currently. In this paper, we design a dynamic-modulated all-dielectric microwave control device to reconstruct the phase profile by filling different dielectric constants of media into it. As a result, the deflection direction of the electromagnetic waves, including whether the deflection occurs or not, can be controlled by this device flexibly. The device with such dynamic modulation function has potential application in the design and development of other functional devices or system, such as switches, beam shaping and imaging systems.

**Index Terms** — All-dielectric metamaterials, beam shaping, dynamic switching.

## I. INTRODUCTION

With the development of science and technology, research on electromagnetic waves control has become more and more significant. There are broad research and application prospects for the wavefront control of electromagnetic waves in imaging, stealth technology, communication technology, electromagnetically induced transparency [1-7], and so on. In recent years, the complete control of the phase, amplitude, and polarization direction of the refracted or reflected electromagnetic waves are studied extensively [8-10]. The amplitude and phase of the electromagnetic waves can be flexibly modulated by the different metamaterial structures and the distribution of the metamaterial unit cells [11-13]. Metamaterials are widely applied to functional electromagnetic waves devices because of their singular

characteristics and have made great progress in practical applications in the field of microwaves. 3D all-dielectric metamaterials devices have attracted lots of interests since the development of 3D printing technology has been maturing [14-17]. Wavefront control devices fabricated by all-dielectric materials have attracted widespread attention for its advantages of low absorption and less expensive, compared with those based on the metal material. A series of electromagnetic waves control devices that used as beam steering devices or lens have been designed [18-20]. Dynamic metamaterials devices are more versatile and flexible compared with normal metamaterials devices to fulfill the demands in the imaging systems, communication systems [21-22]. Part or all areas are filled with dynamically changing materials in metamaterials devices that can enable the devices to be reconfigurable or adjustable, which will be suitable for more demanding applications. Compared to natural materials, all-dielectric metamaterials can achieve arbitrary effective dielectric constants by designing structure or mixing different dielectric constant natural materials in a set of proposed ratios to fulfill the requirements of the control the electromagnetic waves [2,23].

Based on generalized Snell's law, dynamic wavefront control can be achieved by reconstructing the phase profile of metamaterials. In this paper, an all-dielectric microwave control device has been designed to realize dynamic wavefront control. Any phase between 0 to  $2\pi$  can be achieved by the proposed metamaterial unit cells, which enables the dynamic control of electromagnetic waves that has potential applications in microwave beam shaping and imaging.

## II. DESIGN AND SIMULATION OF UNIT CELL STRUCTURE

Reflection and refraction occur when electromagnetic waves are incident on the interface of the medium [8, 24]. It is known from generalized Snell's law that modulation of electromagnetic waves can be achieved

by introducing a gradient phase at the interface. The generalized refractive law formula is as follows:

$$\sin(\theta_t) n_t - \sin(\theta_i) n_i = \frac{\lambda_0}{2\pi} \frac{d\Phi}{dx}, \quad (1)$$

Where  $\theta_i$ ,  $\theta_t$  are the incident and refractive angle,  $n_i$  and  $n_t$  are the refractive indexes of the two media, respectively,  $d\Phi$  is the phase gradient of the two intersections formed by the two optical paths and the interface,  $dx$  is the distance between the two intersections,  $\lambda_0$  is the wavelength of light in vacuum.

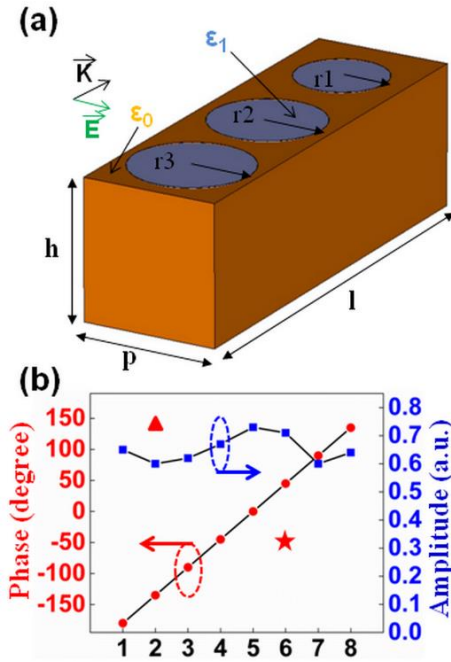


Fig. 1. (a) Schematic diagram of the unit cell (TCCH). (b) Calculated phase shift and amplitude from eight unit cells at 21 GHz. When  $\epsilon_1=1$ , the square and circle represent the amplitude and phase of the eight basic unit cells respectively. When  $\epsilon_1=2.25$ , the phase of Unit\_2 is switched from  $-135^\circ$  to  $135^\circ$  marked as triangle (▲). When  $\epsilon_1=1.44$ , the phase of Unit\_6 is switched from  $45^\circ$  to  $-45^\circ$  marked as pentagram (★).

In order to obtain the phase that can achieve wavefront control, a new subwavelength metamaterials which consists of three combined circular holes (TCCH) is proposed in this paper, as shown in Fig. 1 (a). Three circular holes are designed on the top of the structure to be filled with different media. The material of the structure is nylon (its dielectric constant  $\epsilon=3.6$  and loss tangent  $\delta=0.026$ ) and the medium in the circular holes is air ( $\epsilon_1=1$ ). According to the relationship between velocity of light  $c$ , wavelength  $\lambda$  and frequency  $\nu$ , which is shown as the formula (2):

$$\lambda = \frac{c}{\nu}, \quad (2)$$

To design subwavelength metamaterials, the period

of metamaterial structure has been set less than a wavelength, and its dimensions are as follows: the length, width and height are respectively  $l=25$  mm,  $p=8$  mm,  $h=8$  mm,  $r_1$ ,  $r_2$ ,  $r_3$  represent the radius of three circular holes respectively. In this paper, we use the commercial software CST to study the relationship between radius and phase of metamaterials. The phase is determined by the volume ratios of the two different media in the unit structure, so a complete  $0$  to  $2\pi$  phase change can be realized by changing the radius  $r$  of the circular holes, and the transmission intensity remains relatively stable. The radius of the three circular holes are not set equal to obtain a relatively large phase change as much as possible. Such an asymmetric structural design can reduce the influence of the reflection phase to achieve a large angle deflection of electromagnetic waves [25]. Then eight unit cells are obtained as shown in Table 1. The phase amplitude of eight unit cells is uniform and the step size is  $\pi/4$ , as shown in Fig. 1 (b). Last but not least, the TCCH is flexible and can be made by 3D printing simply.

Table 1: Geometric parameters of the eight TCCH unit cells at 21 GHz ( $\epsilon_1 = \epsilon_{air} = 1$ )

| Unit           | 1    | 2    | 3    | 4    | 5    | 6    | 7   | 8   |
|----------------|------|------|------|------|------|------|-----|-----|
| Phase (degree) | -180 | -135 | -90  | -45  | 0    | 45   | 90  | 135 |
| r1 (mm)        | 1.9  | 1.86 | 2.18 | 2.22 | 2.66 | 3.47 | 0.4 | 1   |
| r2 (mm)        | 1.5  | 1.5  | 2    | 3    | 3.3  | 3.2  | 0.4 | 1.5 |
| r3 (mm)        | 2    | 3    | 3.5  | 3.5  | 3.5  | 3.5  | 0.8 | 1.5 |

Metamaterials are effective EM media with arbitrary dielectric constants, and the effective dielectric constant determines the phase. For dynamic control, it is necessary to introduce phase transition based on the existing structure to realize the reconfigurable and adjustable functions of the device. The relationship of the effective dielectric constant  $\epsilon$ , the dielectric constant of different materials  $\epsilon_a, \epsilon_b$ , and their volume filling rate  $V$  is shown as the following formula [2]:

$$\epsilon = \epsilon_a * V + \epsilon_b * (1 - V), \quad (3)$$

As mentioned above, two different methods can be adopted to reconstruct the phase as we desired. One is to mix materials with different dielectric constants at a specific ratio to obtain a specific dielectric constant, the other is to print structures at different filling rates through 3D printing technology. For instance, when the medium ( $\epsilon_1=2.25$ ) is filled into the circular holes of unit with initial phase  $-135^\circ$ , a new phase  $135^\circ$  can be obtained as shown in Fig. 1 (b). Similarly, while the medium ( $\epsilon_1=1.44$ ) is filled into the circular holes of the unit with initial phase  $45^\circ$ , a new phase  $-45^\circ$  can be obtained. The transmission amplitude remains relatively

stable during this process. Therefore, the purpose of reconfiguring phase can be achieved by filling media of different dielectric constants into circular holes.

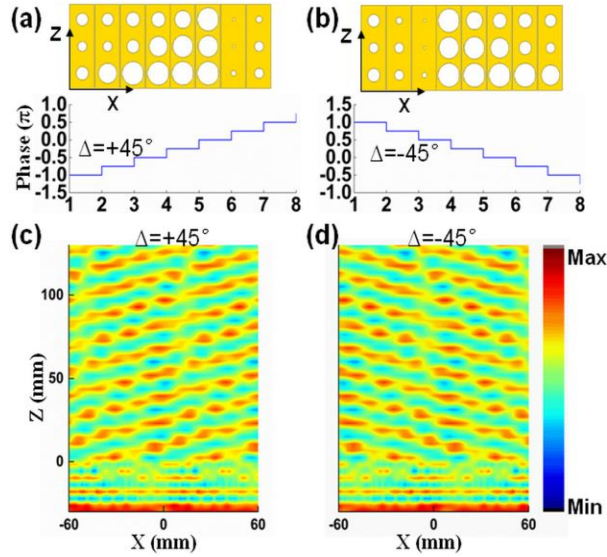


Fig. 2. Eight unit cells with different geometric parameters provide increased phase gradient (a), or provide decreased phase gradient (b). Electric field distribution in the XOZ plane according to a phase gradient of +45° (c) and -45° (d) at 21 GHz.

So as to prove the above generalized law of refraction, a set of arrays based on a combined circular structure is designed. For example, we construct two arrays of cell devices with a phase gradient of 45° (or -45°) in a one-dimensional array, the incident wave is deflected into two different directions, respectively. Here, the eight basic structures we chose were made of nylon and air. Under the incident of electromagnetic waves in the x-polarization direction, the electric field distribution of the device in the XOZ plane is as shown in Fig. 2. The simulation results demonstrate that the control of deflection of electromagnetic waves can be achieved by such devices based on TCCH structures properly.

### III. SWITCHABLE CONTROL OF ELECTROMAGNETIC WAVES

In order to achieve dynamic control, such metamaterials devices are improved by inducing phase transition on the unit structures. What has been proved that when the media are filled into the cell structure, the phase can be reconstructed without changing the size of the cell structure [26]. Here, two basic units (Unit\_2 and Unit\_6) in Table 1 with phase -135° and 45° are selected to reconstruct their phases. As mentioned above, new phases (135° and -45°) can be obtained by filling media with different dielectric constants into the circular holes

of Unit\_2 (phase -135°) and Unit\_6 (phase 45°), respectively. Based on the above conclusions, four coded particles "1", "2", "3", "4" are used to stand for the phases of the transmitted waves of -135°, 135°, -45°, and 45°. In particular, the phase 135° and -45° are reconstructed from the phase -135° and 45°, respectively. To mimic periodic boundary conditions, each of the code phases is on behalf of a super subunit consisting of 3\*3 identical basic unit phases, which minimizes EM coupling between devices with different geometric parameters [13, 27]. Four sequences are designed with two basic coded particles. They are S1 (1144), S2 (2134), S3 (1243), S4 (without phase gradient) which are composed of 36\*36 particles. In the simulation, the boundary in the X, Y and Z directions is set to the open space boundary condition. Then the X-direction polarized wave is incident along the Z perpendicular to the designed device surface. We observe that when the device is arranged according to the basic sequence S1, the 3D far-field scatter plot shows that the normal incident wave is split into two symmetrically distributed beams along the Z-axis, as shown in Fig. 3. It can be seen that two main lobes are symmetrically distributed on both sides of the Z-axis. For the purpose of better visualizing this phenomenon, the two-dimensional scattering pattern in the polar coordinate system and the electric field distribution are given as well. It should be noted that the incident direction of the 3D far-field scatter plot (Fig. 3 (c)) is opposite to that of the electric field distribution diagram (Fig. 3 (d)).

Modulating the phase by filling the media into the super subunits of the first and third columns of S1, we can get the sequence S2 (2134), the phases from left to right are 135°, -135°, -45°, and 45°, respectively. The 3D far-field scatter plot shows that the beam which has just been split into two symmetric distributions along the Z-axis is now suppressed on one side. This phenomenon is also observed in the two-dimensional scattering mode in the polar coordinate system. The electric field distribution is able to clearly observe the deflection of electromagnetic waves. Similarly, modulating the phase by filling the media into the super subunits of the second and fourth columns of S1, we can get the sequence S3 (1243), the phases from left to right are -135°, 135°, 45°, and -45°, respectively. We can observe the opposite phenomenon in S2. But when all the super subunits are filled with the media which have the same dielectric constant as substrate, the sequence S4 can be obtained. Then the phase gradient and the deflection of the electromagnetic waves disappear and the device is equivalent to a transparent window. These four functional devices selected for demonstration are based on the evolution of the two basic unit phases. Therefore, different gradient phase sequences can be constructed based on a set of basic sequences by filling different media into the super subunit structure, so as to control

the deflection direction of electromagnetic waves dynamically.

The method used in this paper for the design of devices is as same as those in the papers which is already

proved effective by experiments [20,25,27-29], so the devices we designed in this paper can also be functional through specific fabrication methods, for example 3D printing.

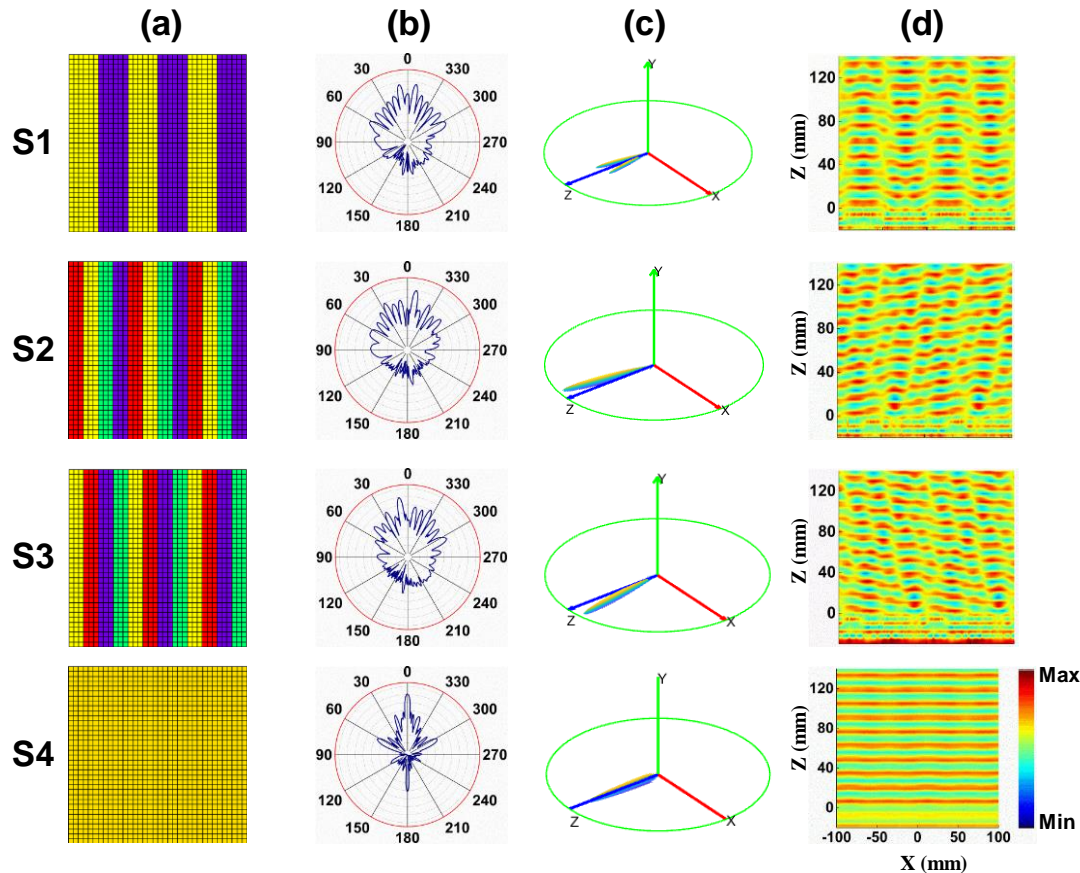


Fig. 3. Geometries of the four sequences and corresponding 2D circular coordinate scattering modes, 3D scattering patterns, and electric field phase distribution of the XOZ plane that are numerically simulated by CST. From top to bottom, S1, S2, S3, and S4 respectively. (a) Schematic representation of four sequences. (b) The 2D circular coordinate scattering modes of four sequences indicating different transmission angles clearly (in logarithmic coordinates). (c) The 3D far-field scattering patterns of four sequences (in linear coordinates). (d) Electric field distribution in the XOZ plane of four sequences.

#### IV. CONCLUSION

In conclusion, an all-dielectric functional device has been designed which enables dynamic wavefront control. The phase of unit cells can be reconstructed by filling different media into circular holes. Four different filling modes are demonstrated to prove that the proposed device can control the deflection direction of the electromagnetic waves, flexibly. Therefore, the all-dielectric metamaterials devices proposed in this paper are low-cost and can be easily printed by 3D printing. The method of dynamic modulation can be freely applied to many devices in the fields for imaging, communications and signal modulation.

#### ACKNOWLEDGMENT

This work was supported by the National Natural Science Foundation of China (No. 61205095), the Shanghai Young College Teacher Develop funding schemes (No. slg11006). The authors gratefully acknowledge Prof. T. J. Cui and Dr. S. Liu from Southeast University for the discussion on simulation method.

#### REFERENCES

- [1] Q. Zhou, P. Liu, D. Yu, L. Bian, and C. Liu, "Field-controlled switchable frequency selective surface with broadband absorption characteristic," *Iet*

- Microwaves Antennas & Propagation*, 2018.
- [2] L. Yin, J. Doyhamboure-Fouquet, X. Tian, and D. Li, "Design and characterization of radar absorbing structure based on gradient-refractive-index metamaterials," *Composites Part B: Engineering*, pp. 178-187, 2018.
- [3] C. M. Watts, X. Liu, and W. J. Padilla, "Metamaterial electromagnetic wave absorbers," *Advanced Materials*, pp. OP98-OP120, 2012.
- [4] J. A. Dockrey, M. J. Lockyear, S. J. Berry, S. A. R. Horsley, J. R. Sambles, and A. P. Hibbins, "Thin metamaterial Luneburg lens for surface waves," *Physical Review B Condensed Matter*, pp. 951-957, 2013.
- [5] J. Zhou, J. Wang, K. Guo, F. Shen, Q. Zhou, Y. Zhiping, and Z. Guo, "High-efficiency terahertz polarization devices based on the dielectric metasurface," *Superlattices and Microstructures*, pp. 75-81, 2018.
- [6] K. Chen, Y. Wang, J. Liu, Y. Bai, T. Bu, B. Cai, Y. Zhu, and S. Zhuang, "Polarization dependent dual-band EIT-like effect and its application in THz range," *Optics Communications*, pp. 69-73, 2016.
- [7] Y. Bai, K. Chen, H. Liu, T. Bu, B. Cai, X. Jian, and Y. Zhu, "Optically controllable terahertz modulator based on electromagnetically-induced-transparency-like effect," *Optics Communications*, pp. 83-89, 2015.
- [8] N. Yu, P. Genevet, M. A. Kats, F. Aieta, J. P. Tetienne, F. Capasso, and Z. Gaburro, "Light propagation with phase discontinuities: Generalized laws of reflection and refraction," *Science*, pp. 333-337, 2011.
- [9] L. Liu, X. Zhang, M. Kenney, X. Su, and N. Xu, "Broadband metasurfaces with simultaneous control of phase and amplitude," *Advanced Materials*, pp. 5031-5036, 2014.
- [10] D. Jia, Y. Tian, W. Ma, X. Gong, J. Yu, G. Zhao, and X. Yu, "Transmissive terahertz metalens with full phase control based on a dielectric metasurface," *Optics Letters*, pp. 4494-4497, 2017.
- [11] Q. Zhang, M. Li, T. Liao, and X. Cui, "Design of beam deflector, splitters, wave plates and metalens using photonic elements with dielectric metasurface," *Optics Communications*, pp. 93-100, 2018.
- [12] Z. Guo, L. Zhu, F. Shen, H. Zhou, and R. Gao, "Dielectric metasurface based high-efficiency polarization splitters," *Rsc. Advances*, pp. 9872-9879, 2017.
- [13] X. Bie, X. Jing, Z. Hong, and C. Li, "Flexible control of transmitting terahertz beams based on multilayer encoding metasurfaces," *Applied Optics*, 2018.
- [14] W. X. Jiang, S. Ge, T. Han, S. Zhang, M. Q. Mehmood, C. W. Qiu, and T. J. Cui, "Shaping 3D path of electromagnetic waves using gradient-refractive-index metamaterials," *Adv. Sci.*, 2016.
- [15] Y. Xie, S. Ye, C. Reyes, P. Sithikong, B. I. Popa, B. J. Wiley, and S. A. Cummer, "Microwave metamaterials made by fused deposition 3D printing of a highly conductive copper-based filament," *Applied Physics Letters*, pp. 788-792, 2017.
- [16] H. Yi, S. W. Qu, K. Ng, C. Chan, and X. Bai, "3D printed millimeter-wave and terahertz lenses with fixed and frequency scanned beam," *IEEE Transactions on Antennas & Propagation*, pp. 442-449, 2016.
- [17] H. F. Ma and T. J. Cui, "Three-dimensional broadband and broad-angle transformation-optics lens," *Nature Communications*, 2010.
- [18] T. Ding, J. Yi, H. Li, H. Zhang, and S. N. Burokur, "3D field-shaping lens using all-dielectric gradient refractive index materials," *Scientific Reports*, 2017.
- [19] J. Yi, S. N. Burokur, G. P. Piau, and A. D. Lustrac, "3D printed broadband transformation optics based all-dielectric microwave lenses," *Journal of Optics*, 2016.
- [20] J. Yi, S. N. Burokur, G. Piau, and A. D. Lustrac, "Coherent beam control with an all-dielectric transformation optics based lens," *Sci. Rep.*, 2016.
- [21] C. Li, J. Wu, S. Jiang, R. Su, C. Zhang, C. Jiang, G. Zhou, B. Jin, L. Kang, and W. Xu, "Electrical dynamic modulation of THz radiation based on superconducting metamaterials," *Applied Physics Letters*, 2017.
- [22] J. M. Manceau, N. H. Shen, M. Kafesaki, C. M. Soukoulis, and S. Tzortzakis, "Dynamic response of metamaterials in the terahertz regime: Blueshift tunability and broadband phase modulation," *Applied Physics Letters*, 2010.
- [23] E. E. Narimanov and A. V. Kildishev, "Optical black hole: Broadband omnidirectional light absorber," *Applied Physics Letters*, pp. 041106-041103, 2009.
- [24] K. Tan, C. Liang, and X. Shi, "Optic eikonal, Fermat's principle and the least action principle," *Science in China Series G: Physics, Mechanics and Astronomy*, pp. 1826-1834, 2008.
- [25] J. Li, C. Shen, A. Díazrubio, S. A. Tretyakov, and S. A. Cummer, "Systematic design and experimental demonstration of bianisotropic metasurfaces for scattering-free manipulation of acoustic wavefronts," *Nature Communications*, 2018.
- [26] P. C. Wu, W. Zhu, Z. X. Shen, P. H. J. Chong, W. Ser, D. P. Tsai, and A.-Q. Liu, "Broadband wide-angle multifunctional polarization converter via liquid-metal-based metasurface," *Advanced Optical Materials*, 2017.
- [27] S. Liu, T. J. Cui, Z. Lei, X. Quan, W. Qiu, W.

Xiang, Q. G. Jian, X. T. Wen, Q. Q. Mei, and G. H. Jia, "Convolution operations on coding metasurface to reach flexible and continuous controls of terahertz beams," *Advanced Science*, 2016.

- [28] M. Wei, Q. Xu, Q. Wang, et al., "Broadband non-polarizing terahertz beam splitters with variable split ratio," *Applied Physics Letters*, vol. 111, no. 7, p. 071101, 2017.
- [29] C. Pfeiffer, N. K. Emani, A. M. Shaltout, et al., "Efficient light bending with isotropic metamaterial Huygens' surfaces," *Nano Letters*, vol. 14, no. 5, pp. 2491-2497, 2014.

**Yanan Hua** received the B.S. degree in Optical Information Science and Technology from Nanjing University of Information Science and Technology (NUIST), Nanjing, China, in 2012. In 2016, she began her M.S. degree in University of Shanghai for Science and Technology (USST). Her research interests include Electromagnetic metamaterials, and 3D printing technology.

**Kejian Chen** is an Associate Professor at University of Shanghai for Science and Technology (USST). He received his B.S. and MPhil. degrees from Zhejiang University, in 2001 and 2004. After completing his Ph.D. in Electronic Engineering in 2009 at The Chinese University of Hong Kong, he worked in Shougang Concord Technology Holdings Limited and the was involved in research efforts at USST from 2011. His research interests include metamaterials; 3D/4D printing and sensors; semiconductor optoelectronic devices, as well as terahertz technologies.

**Yanjuan Fu** received the B.S. degree from Nanjing University of Posts and Telecommunications (NJUPT) in 2017. Since 2017, she became a postgraduate in University of Shanghai for Science and Technology (USST). Her research interests include 4D printing, and shape memory materials.

**Xiaofan Zhang** began her B.S. degree in University of Shanghai for Science and Technology (USST) in 2013. After graduating from the Department of Electro-Optical Engineering, she went on to study for M.S. degree there. Her research interests include metamaterials absorption, and optical fiber transmission.